

DTIC FILE COPY

2

TECHNICAL REPORT BRL-TR-3125

**BRL**

AD-A226 031

LASER-BASED MULTIPHOTON EXCITATION PROCESSES  
IN COMBUSTION DIAGNOSTICS

BRAD E. FORCH  
ANDRZEJ W. MIZIOLEK  
JEFFREY B. MORRIS

JULY 1990

DTIC  
ELECTE  
AUG 30 1990  
E D

CO

APPROVED FOR PUBLIC RELEASE; DISTRIBUTION UNLIMITED.

U.S. ARMY LABORATORY COMMAND

BALLISTIC RESEARCH LABORATORY  
ABERDEEN PROVING GROUND, MARYLAND

90 02 20 176

## NOTICES

Destroy this report when it is no longer needed. DO NOT return it to the originator.

Additional copies of this report may be obtained from the National Technical Information Service, U.S. Department of Commerce, 5285 Port Royal Road, Springfield, VA 22161.

The findings of this report are not to be construed as an official Department of the Army position, unless so designated by other authorized documents.

The use of trade names or manufacturers' names in this report does not constitute indorsement of any commercial product.

# UNCLASSIFIED

REPORT DOCUMENTATION PAGE			Form Approved OMB No. 0704-0188
Public reporting burden for this collection of information is estimated to average 1 hour per response, including the time for reviewing instructions, searching existing data sources, gathering and maintaining the data needed, and completing and reviewing the collection of information. Send comments regarding this burden estimate or any other aspect of this collection of information, including suggestions for reducing this burden, to Washington Headquarters Services, Directorate for Information Operations and Reports, 1215 Jefferson Davis Highway, Suite 1204, Arlington, VA 22202-4302, and to the Office of Management and Budget, Paperwork Reduction Project (0704-0188), Washington, DC 20503.			
1. AGENCY USE ONLY (Leave blank)	2. REPORT DATE July 1990	3. REPORT TYPE AND DATES COVERED Final, Oct 88 - Oct 89	
4. TITLE AND SUBTITLE LASER-BASED MULTIPHOTON EXCITATION PROCESSES IN COMBUSTION DIAGNOSTICS		5. FUNDING NUMBERS  1L161102AH43	
6. AUTHOR(S) Brad E. Forch, Andrzej W. Miziolek, Jeffrey B. Morris			
7. PERFORMING ORGANIZATION NAME(S) AND ADDRESS(ES)		8. PERFORMING ORGANIZATION REPORT NUMBER	
9. SPONSORING / MONITORING AGENCY NAME(S) AND ADDRESS(ES) Ballistic Research Laboratory ATTN: SLCBR-DD-T Aberdeen Proving Ground, MD 21005-5066		10. SPONSORING / MONITORING AGENCY REPORT NUMBER  BRL-TR-3125	
11. SUPPLEMENTARY NOTES			
12a. DISTRIBUTION / AVAILABILITY STATEMENT  Approved for public release; distribution unlimited		12b. DISTRIBUTION CODE	
13. ABSTRACT (Maximum 200 words) Light atomic species such as oxygen atoms (O) and hydrogen atoms (H) are fundamentally important in a wide variety of combustion related phenomena such as flame ignition, propagation, extinction, and in chemical flame reactions. Furthermore, they are difficult to detect by conventional laser based optical methods (laser induced fluorescence) in combustion environments because the necessary resonance excitation wavelengths fall far into the vacuum ultraviolet (vuv) and the requisite tunable laser sources are not generally available. However, recent developments in nonlinear spectroscopic techniques such as multiphoton induced emission (MPE) and multiphoton ionization (MPI) have made direct detection of these light atoms possible. We have utilized a number of laser multiphoton excitation schemes for their detection using tunable lasers in the 190-400 nm range. Similar diagnostic techniques were attempted for the detection of carbon (C) and nitrogen (N) atoms in flames. The effects of laser induced photochemical perturbations on species detection in flames were also investigated. <i>Keywords</i>			
14. SUBJECT TERMS Atoms, Laser Induced Fluorescence, Multiphoton Ionization, Optogalvanic, Flames, Fuel, Oxidizer, Laser, Dye Laser <i>(jbc)</i>		15. NUMBER OF PAGES 33	
		16. PRICE CODE	
17. SECURITY CLASSIFICATION OF REPORT Unclassified	18. SECURITY CLASSIFICATION OF THIS PAGE Unclassified	19. SECURITY CLASSIFICATION OF ABSTRACT Unclassified	20. LIMITATION OF ABSTRACT UL

INTENTIONALLY LEFT BLANK.

TABLE OF CONTENTS

	<u>Page</u>
LIST OF FIGURES.....	v
ACKNOWLEDGEMENT.....	vii
I. INTRODUCTION.....	1
II. EXPERIMENTAL SECTION.....	3
III. RESULTS AND DISCUSSION.....	5
A. O-Atoms.....	5
B. H-Atoms.....	13
C. N- and C-Atoms.....	18
IV. CONCLUSION.....	18
REFERENCES.....	21
DISTRIBUTION LIST.....	23

Accession For	
NTIS GRA&I	<input checked="" type="checkbox"/>
DTIC TAB	<input type="checkbox"/>
Unannounced	<input type="checkbox"/>
Justification _____	
By _____	
Distribution/ _____	
Availability Codes	
Dist	Avail and/or Special
<b>A-1</b>	

INTENTIONALLY LEFT BLANK.

## LIST OF FIGURES

<u>Figure</u>	<u>Page</u>
1	Experimental Schematic for Flame Diagnostic Work.....4
2	Simple Energy Level Diagram for Oxygen Atoms.....6
3	Excitation Spectrum for the Oxygen Atom Emission at 845.7 nm from Primary Reaction Zone of an H <sub>2</sub> /O <sub>2</sub> Atmospheric Pressure Flame.....7
4	(a) Temporal Profile of the Exciting UV Laser Light at 225.6 nm (Scattered Pulse), (b) The Oxygen Atom Emission in an Atmospheric Pressure H <sub>2</sub> /O <sub>2</sub> Flame ( $\lambda=777.5$ nm), and (c) The Temporal Profile of the Microplasma Emission ( $\lambda=777.5$ nm).....8
5	(a) Oxygen Profile Atom in an H <sub>2</sub> /O <sub>2</sub> Atmospheric Pressure Flame and (b) Same Profile Taken at Higher Laser Energy and Shorter Focal Length Lens as Described in the Text.....10
6	(a) Excitation Spectrum (Emission) of O Atoms from the Photolysis of O <sub>2</sub> in a Cold Flow, and (b) The Excitation Spectrum (MPI) Taken With the Optogalvanic Probe Under the Same Experimental Conditions.....11
7	Plot of the Incident Laser Energy Required to Ignite a Premixed Flow of H <sub>2</sub> /O <sub>2</sub> as a Function of Laser Wavelength in the Region of 226 nm.....13
8	Simple Energy Level Diagram and Multiphoton Excitation Schemes for H Atoms.....14
9	(a) Excitation Spectrum for H Atoms Using the Three-Photon Excitation ( $\lambda=272$ nm) Scheme 5 as Depicted in (b).....16
10	Mass-Gated Ion Signals (Excitation Spectrum) of H <sup>+</sup> and D <sup>+</sup> Taken in a Time-of-Flight Mass Spectrometer.....17

INTENTIONALLY LEFT BLANK.

## ACKNOWLEDGEMENT

This work was supported in part by the Air Force Office of Scientific Research (AFOSR), Directorate of Aerospace Sciences, Contract Number 88-0013 and 89-0017 and in-house laboratory research funding (ILIR). Special thanks go to Professor T.A. Cool for the design and construction of the optogalvanic probe used in this work.

INTENTIONALLY LEFT BLANK.

## I. INTRODUCTION

Light atomic species such as oxygen and hydrogen atoms are fundamentally important in a wide variety of combustion processes such as flame ignition, propagation and extinction and in chemical flame reactions. The hydrogen atom/radical, for example, is necessarily important in nearly every combustion process because of its high reactivity and diffusivity, yet its direct detection therein is very difficult. The oxygen atom is of equal importance in pertinent flame processes, flame structure and relevant chemical and mass transfer processes but its direct detection is equally difficult. The nitrogen atom is a constituent of many gaseous, liquid and solid oxidizers (of particular importance to the chemistry of propellant combustion) since it is chemically bound in nitrate, nitro and nitroso compounds, but has never been detected in a flame environment (to our best knowledge). Conventional optical detection of these light atoms is difficult for a variety of reasons. In particular, the necessary optical resonance excitation wavelengths fall far into the ultraviolet (uv) and the requisite tunable laser sources are generally not available for such flame atomic spectroscopy. For example, the lowest lying resonance states for oxygen and hydrogen atoms lie in the wavelength region of  $< 140$  nm. Likewise, carbon and nitrogen atom resonance transitions ( $< 130$  nm) lie in the vacuum ultraviolet (vuv) spectral region, which makes flame spectroscopy very difficult as these wavelengths are absorbed strongly by atmospheric gases (particularly  $O_2$ ). Historically, several different laser spectroscopic techniques have been employed for both detection and diagnostics of these light atoms in combustion processes.<sup>1-7</sup> One of the most successful methods thus far for flame diagnostics has been laser-induced fluorescence (LIF) primarily because it can yield spatially resolved measurements with a high degree of sensitivity.<sup>3</sup> Since the energy gap between the ground and excited electronic states of the light atoms is typically on the order of 10 or more electron volts (ev), techniques such as two-photon or multiphoton laser excitation methods must be employed. Under high laser intensity (typically using a focused beam of a pulsed laser) two or more laser photons may be absorbed through virtual states, which are not eigenstates of the absorber. Even though these non-stationary states can not retain energy, the assumption may be made that the atom remains for some finite time in the virtual state, typically on the order of  $10^{-15}$  sec. Thus, for absorption to occur on the order of  $< 10^{-15}$  sec, the photon flux must indeed be very great. Such high flux levels are achieved with the use of high peak-power lasers. Multiphoton excitation of these species can therefore be conveniently provided with commercially available laser sources that can quite easily generate the "one-step" photons that may be used in the "multi-step" excitation process.

The advent of tunable, narrow-linewidth lasers has also enabled the development of another multiphoton technique for the detection of and quantification of species such as light atoms, namely multiphoton ionization (MPI).<sup>8,9</sup> Similar to multiphoton laser induced fluorescence experiments, ionization of the atom can be achieved if the energy of the total number of photons which are absorbed is sufficient to eject an electron from the target species, i.e., greater than the ionization potential (IP). Consequently, the "free electrons" which are liberated or positive ions which are produced are amenable for detection. Flame atomic species have been detected, as such, with resonant multiphoton optogalvanic spectroscopy.<sup>4-7</sup> In general, the term optogalvanic loosely refers to changes in the electrical properties of the

environment (the flame) because of photoionization or ionization due to collisions involving highly excited states that have been optically populated.<sup>4</sup> Optogalvanic signals are detected in our laboratory using a platinum tipped probe (described in the experimental section of this paper) which is a point source detector and well suited for spatial measurements in combustion environments. Ultimately the ionization signals are related to relative species densities in flames and if properly calibrated, to absolute concentrations. A particular advantage of optogalvanic detection over LIF is that dark or non-emitting species may be studied. However, both the MPI and MPE approaches suffer from limitations. MPE inherently suffers from quenching considerations and signal collection inefficiencies. A recent paper by Meier, et al.,<sup>10</sup> addresses this issue by measuring the efficiency of fluorescence quenching by the various species present in the detection region. They used a versatile discharge-flow system for the determination of quenching rate constants for the relevant species in flame gases. A method for determining the number densities of H and O atoms in flames was developed using two-photon laser excited fluorescence, which attempted to account for the influence of fluorescence quenching. Aside from quenching considerations, the technique of MPI, in comparison, lacks selectivity in signal detection and thus is quite susceptible to background ionization.<sup>3</sup> There also exists the possibility of introducing perturbations as a result of inserting the probe into the flame medium. Furthermore, multiphoton excitation techniques for flame light atoms may suffer from complications which arise from laser photolysis due to the uv wavelengths, tight beam focusing and high peak laser powers which are required and utilized to drive the highly non-linear processes.<sup>11</sup> We have reported in our laboratory findings which have shown that at sufficiently high laser energies, the flame diagnostic probe can become substantially intrusive by promoting multiphoton dissociation of the parent fuel and oxidizer molecules to produce artificially high concentrations of atomic species (relative to that normally found in a flame environment).<sup>11</sup> This dissociation can lead to potentially erroneous concentration measurements and flame profiles. Two other diagnostic techniques have been used for direct detection of atomic species, namely Raman scattering<sup>12</sup> and coherent anti-Stokes Raman spectroscopy.<sup>13</sup> Both have been employed for flame detection and diagnostics, but suffer from sensitivity limits and other spectral interferences that have prevented further development of these spectroscopies for atomic flame detection.

We are particularly interested in the application of lasers for detailed flame chemistry studies and have been in the process of building up a comprehensive and well-equipped research program in this area. This paper presents an extension on our previous work in light atom diagnostics. We have applied the techniques of MPE and MPI to a variety of flames, in particular  $H_2/O_2$ ,  $H_2/air$ ,  $H_2/N_2O$ ,  $C_2H_2/O_2$  and  $C_2H_2/air$ , for the purpose of further development and implementation of diagnostic techniques for small atomic species such as H, O, C, and N in combustion environments. A great deal of information on, and insight into the details of the various excitation processes can be gained by measuring laser power dependencies. These power dependencies were measured for the photoexcitation of O atoms in  $H_2/O_2$  and  $H_2/N_2O$  flames as well as for the photolytic production and photoexcitation of O atoms in cold flows of the oxidizer components of these flames. Similar investigations were performed on H atoms. Laser power dependencies were measured for the photoexcitation of hydrogen atoms in atmospheric pressure flames and in a molecular-beam time-of-flight mass spectrometer. In the

course of our experimental work we have also become very sensitive to the potentially intrusive nature of the focused laser as a flame diagnostic probe due to photochemical effects caused by the intense uv pulses. We will discuss the effect of photochemical perturbations introduced by lasers in light of our combustion diagnostic work on oxygen atom; in particular, as related to  $H_2/O_2$  premixed flames and reactive gaseous flows. We have investigated the potential utility of the photolytic nature of the focused uv laser with applications to ignition and combustion enhancement by resonant multiphoton photochemical means.<sup>14,15</sup>

## II. EXPERIMENTAL SECTION

A schematic of the experimental set-up for the flame diagnostic work is given in Figure 1. Tunable laser radiation was provided by a 10 Hertz Quanta-Ray Q-switched Nd:YAG-pumped dye laser system (DCR-2A, PDL-1) which is equipped with a wavelength extension system (WEX-1). The WEX-1 is a servo-motor based tracking system which houses two modules which contain non-linear crystals (angle-cut KDP) that are used to frequency double the dye laser output and frequency mix it with the fundamental (1064 nm) of the Nd:YAG to generate tunable wavelengths in the deep ultraviolet (uv). The unwanted beams were separated from the desired uv beam with a Pellin-Broca prism, broad-band filters and an aperture. Typical outputs from the laser system are: two millijoules (mJ) of uv energy at 226 nm using a doubled rhodamine 590 dye and mixed (two-photon excitation of O atoms,  $2p^3 \rightarrow 3p^3P + 2p^4 \rightarrow 3P$ ), one mJ at 243 nm, using a doubled DCM dye and mixed (two photon excitation of H atoms,  $n=1 \rightarrow 2$ ), 10 mJ at 292 nm, using a double Kiton Red dye (three-photon excitation of H atoms  $n=1 \rightarrow 4$ ), 15 mJ at 308 nm, using an acid shifted (HCl) Rhodamine 640 dye (three-photon excitation of H atoms  $n=1 \rightarrow 3$ ), 5 mJ at 365 nm, using a base shifted (saturated NaOH) Fluorescence 548 and mixed (three photon excitation of H atoms  $n=1 \rightarrow 2$ ) and 70  $\mu$ J at 193.1 nm, doubled Kiton-Red, mixed and second anti-Stokes  $H_2$  Raman-shifted (one photon excitation of carbon atoms  $1D_2 + 1P^0_1$ ). The measured laser linewidth in the uv was  $2.2 \text{ cm}^{-1}$  with a temporal width of about 5 nsec. The pulse energy was measured with a Scientech volume-absorbing disc calorimeter (Model 38-0103) and analog meter.

A simple atmospheric pressure jet burner system was fabricated from a Swagelock 0.635-cm stainless steel terminator fitting through which a 0.5 mm hole was drilled. The burner tip was threaded onto a 10 mm stainless steel tube. The fuel and oxidizer were premixed in the burner and the gas flow was regulated by Matheson (Model 620) flowmeters and metering valves that were calibrated with a GCA Precision Scientific wet test meter. For  $H_2$  and  $O_2$ , flows up to 2 liters/min were used which resulted in linear flow velocities in the  $10^3$ -cm/sec range. The burner was equipped with a water cooling jacket and shroud of inert argon gas which encircled the flame and minimized mixing with air and recirculating flow. The burner was mounted on a xyz-translation stage and could be manipulated with micrometer positioners. The laser beam (diameter of 7.5 mm) was focused into the flame or gaseous flow with 50 to 500 mm focal length lenses (25 mm diameter). The estimated focal spot diameter size was 50 to 100  $\mu$ m. The lenses were also similarly mounted in xyz-translation stages. The laser induced fluorescence was collected at right angles to the exciting light with a pair of fused silica biconvex lenses and imaged onto the adjustable slits of a 0.22 m McPherson monochromator (Model 218) which were shielded with the appropriate broad-bandpass and/or interference filters. Fluorescence excitation scans were recorded by tuning

the monochromator to a particular emission wavelength of an atomic or molecular species of interest and scanning the tunable laser through the electronic resonance transition(s). Dispersed fluorescence spectra were recorded by tuning the laser to the appropriate excitation wavelength and then scanning the monochromator through the emission wavelength(s). The photomultiplier (Hamamatsu R928 or EMI 9659QA) signal was then fed to either a Princeton Applied Research or Stanford Research Systems (SRS) boxcar integrator then plotted on a strip-chart recorder, or fed to either a (model 7912AD) Tektronix transient digitizer (500 MHz) or Hewlett Packard (Model 54111D) digital oscilloscope (500 MHz) in order to capture the temporal profile of the emission. Adjustable time delays for synchronization of the detection electronics with the laser were accomplished with a digital pulse-delay generator, either a BNC Model 7085 or SRS Model DG535. Excimer laser radiation (at 193 nm) was provided by either a Lumonics Hyper-EX Model 440 or Model TE 860 both of which were operated in the unstable resonator mode which yields much less divergent laser beams and narrower focused beam waists than in the stable resonator mode.

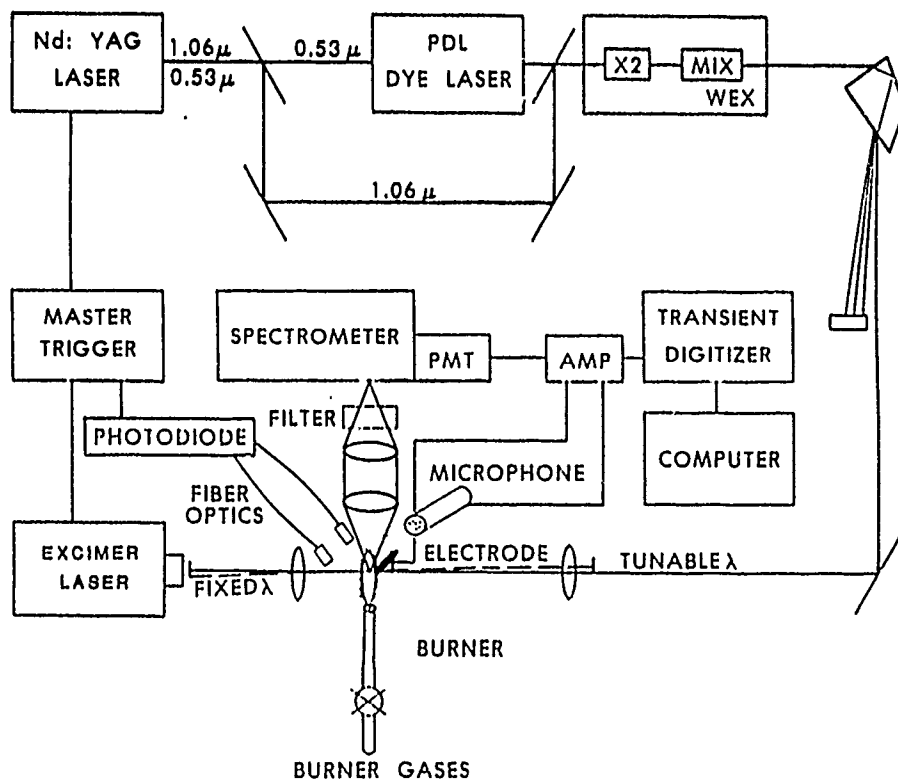


Figure 1. Experimental Schematic for Flame Diagnostic Work

Ions of both atomic and molecular species were detected at atmospheric pressure using an optogalvanic probe which could be forward biased to detect electrons liberated in the laser induced multiphoton photoionization process or reversed biased to detect the resultant positive ionic species. The probe was designed, constructed, characterized and supplied by Professor Terrill A.

Cool of Cornell University.<sup>7</sup> The probe tip is a 1 mm platinum bead (anode) for collecting electrons. The bias voltage between the anode and platinum wire cathode could be adjusted continuously to the point of saturation (about 200 volts) of the electron collection wherein a major fraction of the photo-produced electrons could be detected. Here the saturated probe signal is proportional to the density of the photoionized species over at least four orders of magnitude. At low probe voltages a portion of the signal was lost (due to electron attachment or recombination before reaching the anode) and at higher probe voltages avalanche ionization occurred. Signals on the order of 10's of mv were observed when either differentially amplified using a PAR differential amplifier or AC coupled into a Keithly (Model 427) current amplifier. The ionization signal reaches a peak value in about 2  $\mu$ sec and decays with a single exponential time constant which is established by the RC time constant of the circuit used (about 21  $\mu$ sec). Signals from positive ions were observed on millisecond time scales and were easily discriminated from electron signals.

Mass spectra were recorded with an R.M. Jordan time-of-flight mass spectrometer. The system is equipped with a pulsed-molecular beam valve and is backed by two rotary direct drive pumps, a 10 inch diffusion pump and a 6 inch turbomolecular pump and could be operated near  $10^{-8}$  torr. Pulsed-beams of 30  $\mu$ sec temporal duration could be generated while maintaining a chamber operating pressure of  $10^{-7}$  torr. All gases used in these experiments were prepurified and used as is without further purification.

### III. RESULTS AND DISCUSSION

#### A. O-Atoms

MPE. Two-photon absorption from a uv laser beam to excite ground state oxygen atoms to the first excited state of identical spin symmetry was first reported by Bischel, et al.<sup>17</sup> They described a scheme which is illustrated in Figure 2. The photoexcited  $^3P$  state ( $2p^3 3p \ ^3P \rightarrow 2p^4 \ ^3P_2$ ) can radiate in the near infrared (at 844.7 nm) to the  $^3S$  state, which is a useful analytical wavelength for the detection of the emission. The experiments were performed in a low pressure discharge which produced oxygen atoms in their ground electronic state. The radiative lifetime (39 nsec) and quench rate with  $N_2$  ( $2.5 \times 10^{-10} \text{ cm}^{-3} \text{ sec}^{-1}$ ) were measured. From the results of their experiments they indicated that there was promise for the method as a diagnostic technique for O atoms in flames and plasmas. Subsequently, oxygen atoms were first detected in a realistic combustion environment by Alden, et al., utilizing this scheme.<sup>2</sup> The experiments were performed in fuel lean acetylene/oxygen flame (equivalence ratio of 0.57, temperature = 3000 K). They reported that at this temperature the ground state contains about 60% of the atoms and calculated an oxygen atom mole fraction of around 0.05%. This value was determined to be low in light of the theoretically predicted concentration of 10%: the reason for this discrepancy is not known. They determined the laser power dependence  $n$  which is a measure of the number of photons involved in the excitation process and obtained a value of  $n = 2.6 \pm 0.2$  from the fitted slope of a log-log plot of signal intensity versus laser energy. The expected power dependence should be near quadratic. A value of 1 to 2 would have been obtained if there were a competing process such as saturation of the two-photon transition or rapid photoionization from the excited  $^3P$  state, although there was no evidence as such reported in their work.

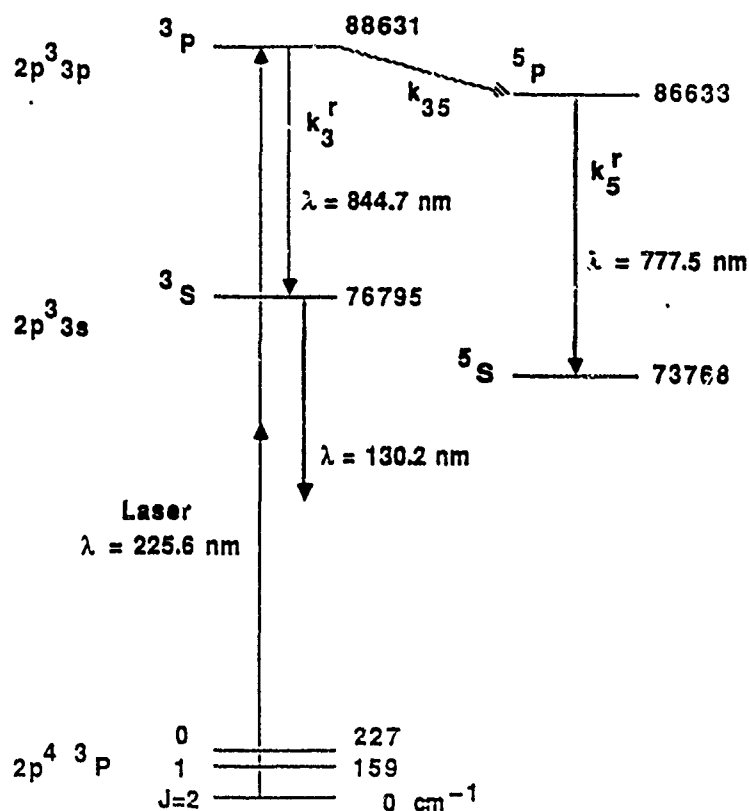


Figure 2. Simple Energy Level Diagram for Oxygen Atoms.  
Terms are defined in the text.

We have also utilized this excitation scheme for oxygen detection in our experimental work.<sup>11,14-16</sup> Figure 3 gives the fluorescence excitation scan of ground state 0 atoms in the primary reaction zone of a premixed stoichiometric ( $\phi=1.0$ )  $H_2/O_2$  atmospheric pressure flame (using a 300 mm focal length lens and the laser energy was 0.4 mJ). The ground spin-orbit split states,  $J=0, 1, 2$  are clearly resolved although the excited state splittings were not resolved with the resolution of our laser system. Signals were not normalized to the intensity profile of the doubled and mixed dye laser beam in this experiment due to the nonlinear nature of the transition. The signal to noise ratio was excellent (100:1). The signal strength was found to be highly sensitive to the flame reaction zone that was probed. The signals were strong, although heavily quenched, and followed the temporal profile of the exciting laser beam, Figures 3a and 4b. We measured the laser power dependence for the process (by either varying the gain of the amplifier stage of the Nd:YAG laser or inserting quartz plates into the 226 nm beam to attenuate the energy) and found that there was a quadratic dependence, i.e.,  $n = 1.9 \pm 0.2$  (the uncertainty was obtained from the standard deviation of the mean from three measurements). We did indeed find that at higher laser energies ( $> 0.4$  mJ) and with a shorter focal length lens we could easily saturate the two-photon transition and also drive higher order nonlinear process such as photoionization of atomic oxygen and photolysis of the parent fuel and oxidizer. Experiments were also performed in a premixed  $H_2/N_2O$  and  $H_2/air$

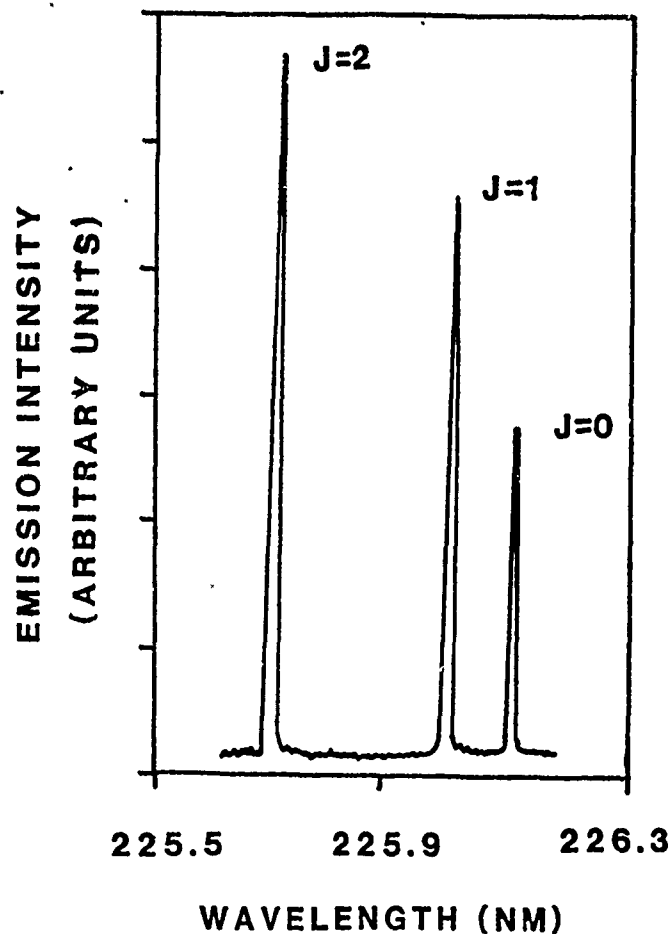


Figure 3. Excitation Spectrum for the Oxygen Atom Emission at 845.7 nm from Primary Reaction Zone of an  $H_2/O_2$  Atmospheric Pressure Flame. The spin-orbit split ground states ( $J=0,1,2$ ) are resolved.

flames and identical experimental results were obtained. Fluorescence spectra were also obtained using a scanning monochromator with the exciting laser light tuned to either of the three oxygen atom ground spin-orbit split states. As previously reported, there was a strong collisional energy transfer to the  $^3P$  state of oxygen with detectable fluorescence emission at 777.5 nm which was also utilized to perform similar diagnostic measurements.<sup>11</sup> Stronger signals were obtained at this emission wavelength in the aforementioned flames, but when the spectral sensitivity of the detection system (monochromator and photomultiplier) were corrected using a calibrated standards lamp, it was found that the signal strength from the 844.7 nm emission was larger.

MPI. Atomic oxygen was also detected in these flame environments using an optogalvanic probe. Here the probe was inserted into the flame itself and the laser was focused within  $<0.5$  mm of the platinum anode of the detector (the burner head itself was grounded). An excitation scan was recorded by scanning the laser through the three ground spin-orbit split states while

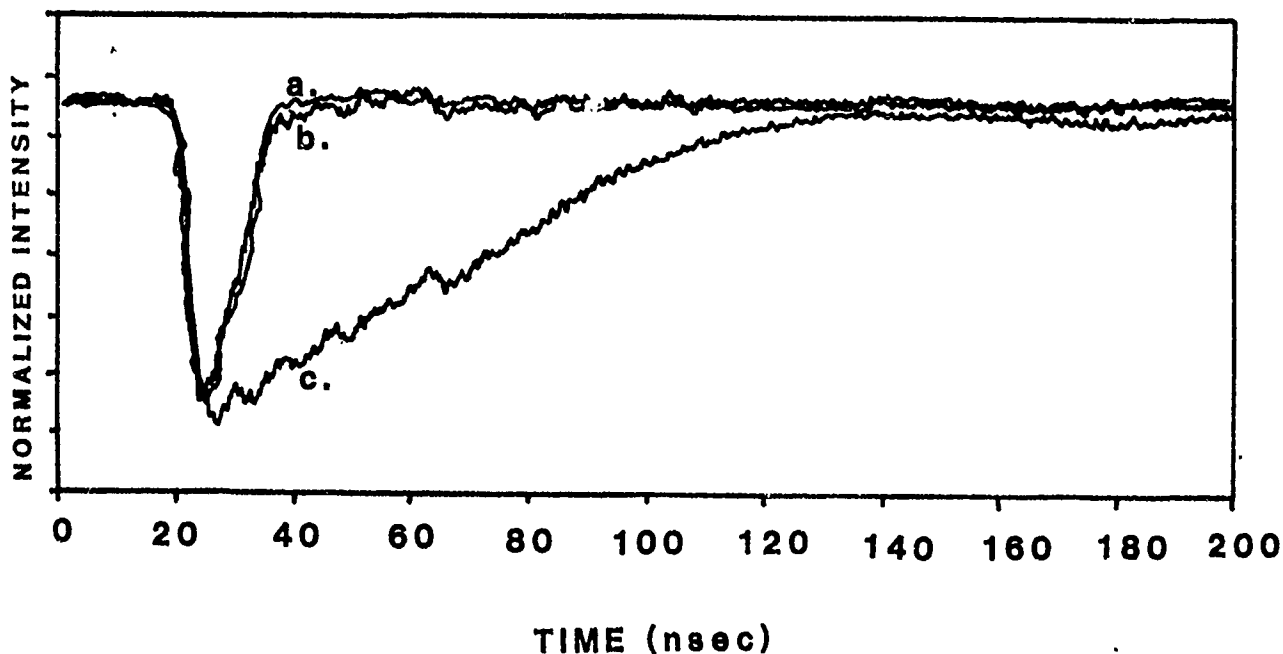


Figure 4. (a) Temporal Profile of the Exciting UV Laser Light at 225.6 nm (Scattered Pulse), (b) The Oxygen Atom Emission in an Atmospheric Pressure  $H_2/O_2$  Flame ( $\lambda=777.5$  nm), and (c) The Temporal Profile of the Microplasma Emission ( $\lambda=777.5$  nm)

using the probe in the forward biased mode where free electrons which were liberated in the photoionization process could be collected (the spectrum was identical to the emission scan in Figure 3). It was found that the signal strength strongly depended on the distance  $r$  of the probe apode to the laser focal spot and that the intensity varied roughly with a  $1/r^2$  dependence ( $r$  was varied from 0.5 to 2 mm while the probe voltage was held constant at 200 V). The laser power dependence for the process was measured as described earlier. At low laser energy (0.1 to 0.5 mJ) we observed a slope of  $2.8 \pm 0.3$  for  $n$  which is indicative of an overall three-photon photoionization process. At higher laser energy (0.6 to 1.2 mJ) a value for  $n = 2.1 \pm 0.2$  was obtained which probably indicates saturation of the two-photon step in the 2+1 resonance ionization process. A similar saturation effect was observed by us in our hydrogen atom work as well as recently by Downey and Hozack<sup>18</sup> who observed  $n$  change from 3.2 to 2 in a 2+1 photoionization process at power densities of near  $10^7$  W/cm<sup>2</sup>. They reasoned that in most 2+1 resonance ionization processes where the real intermediate states enhance the two-photon cross section, saturation of the two-photon excitation step usually occurs at lower intensities than does the ionization step. Similar experiments in our laboratory were performed with the probe bias reversed to detect ions that were formed in the photoionization process and comparable results were obtained. In either case it was found that background signals were negligible, but some RF interference was picked up from the laser power supply through the probe. This noise was largely eliminated when the current amplifier which was used with the the probe was shielded from RF pick-up. Principal reasons for utilizing the optogalvanic probe as a diagnostic tool

for flame detection of atomic species such as O at  $\mu\text{s}$  is the high degree of spatial resolution and sensitivity that it provides, as well as the capability for looking at dark or non-emitting species. Normalized intensity profiles of atomic oxygen could be made quite easily by fixing the spatial position and relative geometric location of the probe tip and the laser focus, and then translating the flame through this area with a precision micrometer drive stage. Resolution on a submillimeter scale could thus be obtained. A chief disadvantage of the probe used in these experiments (aside from the potential intrusive nature of the insertion of any physical element into a flame) is that the platinum anode is subject to deterioration at temperatures  $> 1500$  K. A similar probe is being designed which will be constructed of tungsten and can withstand much higher temperature flame environments.

Photolytic Effects. Earlier experimental results from our laboratory first indicated that in diagnostic work on oxygen atom detection in a flame environment there was evidence that the focused uv laser and high peak powers that were used led to laser induced multiphoton photolysis of the parent oxidizer molecule  $\text{N}_2\text{O}$ , yielding unusually high concentrations of oxygen atoms (higher than that which would normally be found in a combustion environment).<sup>11</sup> The manifestation of this phenomenon, which also occurs in  $\text{O}_2$ -containing systems, is clearly illustrated in Figure 5 which gives a normalized intensity profile of atomic oxygen atoms in a premixed  $\text{H}_2/\text{O}_2$  flame ( $\phi=0.8$ ). In Figure 5a, the laser was tuned to and fixed at the  $J=2$  ground spin-orbit split state; the observation wavelength was 777.5 nm, a 300 mm focal length lens was used and the laser energy was 0.35 mJ. Each data point represents the running average of 64 laser shots acquired with a digital oscilloscope. It was found that the signal intensity was very sensitive to the positioning of the laser focal spot within the flame environment and reached a maximum at a distance of 3.5 mm above the burner head (the starred point in Figure 5), which was the location of the primary reaction zone, then rapidly fell away as the probe region was translated into the post-flame gases. In Figure 5b, the same experiment was then repeated, however this time a shorter focal length lens was used (100 mm) and the laser energy was increased to 0.8 mJ. Very large signals were observed throughout the flame structure. However, as the the sampled flame region was translated into the post-flame gases it was found that the O atom signal intensity did not drop off rapidly as it had in the previous experiment, Figure 5a. Apparently, the focused uv laser beam was inducing the photodissociation of molecular oxygen to produce excess quantities of atomic oxygen. Furthermore, in a darkened laboratory when a tighter focusing lens was used (50 mm) it was quite evident that the formation of a tiny microplasma was being induced, and in addition a faint acoustic report was audible. (We have utilized photoacoustic techniques as diagnostic but will not discuss them here). Even when the laser energy was attenuated to the point wherein microplasma formation was not evident, it was found that relatively high O atom signal intensities could be found. It is known that molecular oxygen does not absorb substantially at wavelengths  $> 200$  nm at room temperature.<sup>19</sup> However, at these flame temperatures (post-flame gas temperature of ca. 1500 K)  $\text{O}_2$  ground state vibrational levels are thermally populated such that single photon excitation at 226 nm through these states (Schumann-Runge bands) which are highly predissociative can lead to the production of excess quantities of O atoms which subsequently may be two-photon excited and emit. As stated before, the laser power dependence for the photolytic process gave a value of  $n=2$ . A power dependence was not measured in the post-flame gases but we suspect that at low laser energies when the

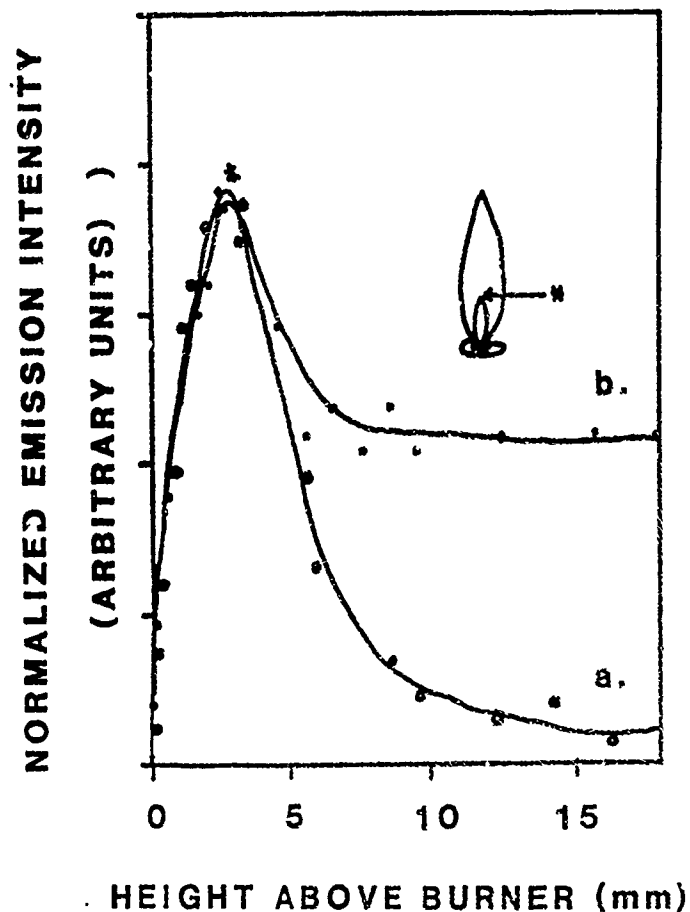


Figure 5. (a) Oxygen Profile Atom in an  $H_2/O_2$  Atmospheric Pressure Flame and (b) Same Profile Taken at Higher Laser Energy and Shorter Focal Length Lens as Described in the Text. The starred point (\*) indicates the location of the primary reaction zone.

two-photon excitation process was not saturated a value of  $n=3$  would be obtained: one photon for a single step photolysis and two-photons for excitation. Subsequent to our single laser experiments, Goldsmith recently described a two-laser experiment where he scanned across molecular-oxygen Schumann-Runge bands at 221 nm in a flame environment and monitored O atom production with a second laser tuned to the  $J=2$  state at 225.6 nm and found a similar photolytic production of excess quantities of atomic oxygen.<sup>20</sup>

We have noted in our flame diagnostic work, not only the photolytic production of O atoms in flames, but also in cold gas flows of  $O_2$ ,  $N_2O$  or air when no flame was present at all. Apparently, the focused laser was inducing the photolysis of these gases to produce ground state oxygen atoms which could then be easily two-photon excited and emission could be detected at 777.5 or 844.7 nm. Figure 6a gives an excitation spectrum of O atoms from the photolysis of  $O_2$  in a cold flow of  $O_2$  (a similar result was obtained with air or  $N_2O$ ). We decided to determine the laser power dependence  $n$  for the process by measuring the signal intensity as a function of laser energy in the cold

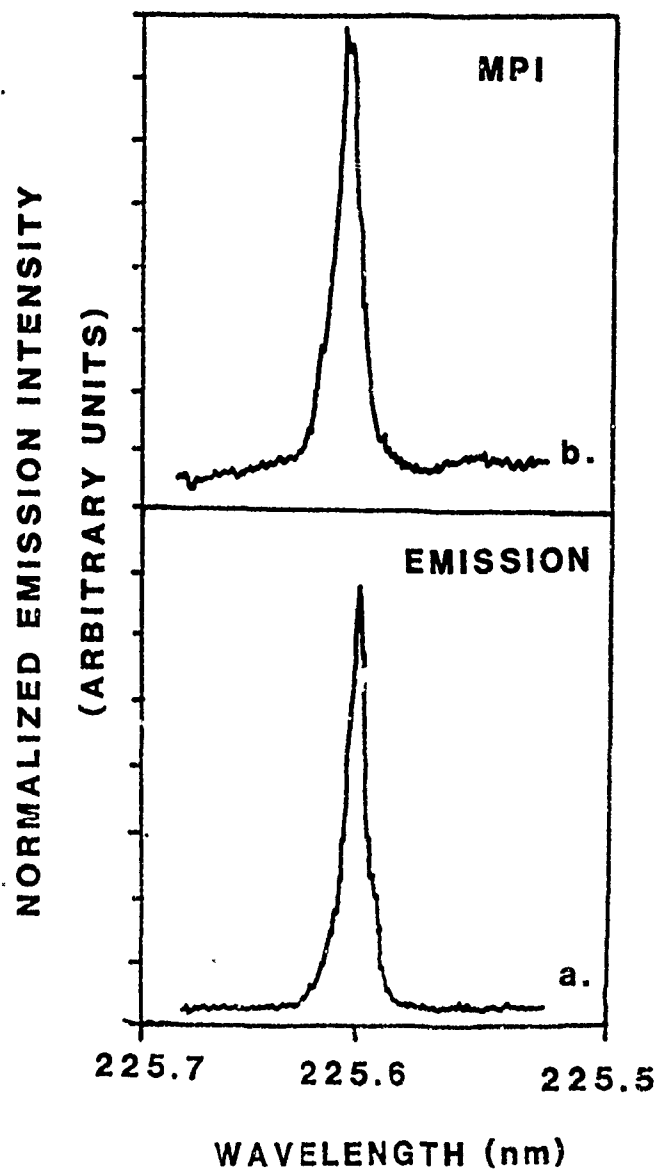


Figure 6. (a) Excitation Spectrum (Emission) of O Atoms from the Photolysis of O<sub>2</sub> in a Cold Flow, and (b) The Excitation Spectrum (MPI) Taken With the Optogalvanic Probe Under the Same Experimental Conditions

flows. We obtained a value of  $n = 3.4 \pm 0.3$  for an O<sub>2</sub> flow and a similar value for an N<sub>2</sub>O flow. Since we have already measured a power dependence of  $n=2$  for the two-photon excitation of atomic oxygen, this result suggests that a two-photon process is responsible for the photolytic production of atomic oxygen from either O<sub>2</sub> or N<sub>2</sub>O in a room temperature flow. The actual value obtained is  $n = 3.4 - 2.0 = 1.4$  (the non-integer value is most likely due to some saturation of the two-photon excitation photolysis processes and/or losses due to rapid photoionization which competes with the fluorescence). Losses due to rapid photoionization have been substantiated by performing the same

measurements utilizing the optogalvanic probe in the flow environment. Under these experimental conditions there were free electrons or positive ions that could be detected with the properly biased probe. Figure 6b gives the excitation spectrum of O atoms taken with the optogalvanic probe (free electrons or positive ions were collected in each scan respectively). At low laser energies we measured a value of  $n = 4.3 \pm 0.3$  for the overall process: photolysis of  $O_2$  to produce O atoms (two photons), photoexcitation of O atoms (two photons) and the photoionization of O atoms (1.0 photons) to yield detectable electrons. The overall process probably requires 5 photons (not 4.3) because the photoexcitation or ionization step may have been partially saturated.

Microplasma Formation. The experimental results in the above section clearly indicate that laser photolysis effects can potentially lead to erroneous measurements of species profiles in combustion environments. We can, however, utilize the photolytic behavior of focused uv lasers to enhance combustion related phenomenon such as ignition augmentation of reactive gaseous flows. We have demonstrated that there are indeed wavelength specific interactions with parent fuel and oxidizer photofragments that lead to resonant ionization, the liberation of free electrons within the laser focal volume and ultimately the formation of a laser produced microplasma.<sup>14,15</sup> We have investigated the feasibility of the utilization of these laser produced microplasmas as a technique for the initiation of combustion events and have studied in some detail the chemistry and mechanism involved in this process. Specifically, we have used the uv laser as an ignition source for premixed  $H_2/O_2$  and  $H_2/N_2O$  flows at atmospheric pressure. This was the first report of such a strong and sensitive wavelength dependence for the initiation of combustion in a reactive gaseous flow. A sharp wavelength dependence on the amount of incident laser energy required to ignite these mixtures was reported. The wavelength dependence, Figure 7, exhibits a spectral profile similar to the two-photon excitation curve for flame oxygen atoms, Figure 3. Figure 7 gives the amount of incident laser energy (ILE, the energy measured before the focusing lens) required to initiate the combustion event as a function of laser wavelength. Ignition occurred within the shaded areas. The respective peaks correspond exactly to the same spectral positions as the oxygen atom two-photon wavelengths near 225.6 nm. Clearly, oxygen atom production and subsequent excitation is an important step in the efficient ( $\sim 0.5$  mJ ILE required) laser ignition of  $H_2/O_2$  flows in this wavelength region. Time resolved measurements were performed on  $O_2$  and  $N_2O$  flows alone and it was found that the resonant formation of a microplasma (with a lifetime on the order of 100 nsec, see Figure 4c.) was responsible. A new combustion initiation phenomenon was discovered which involves atomic resonances in the uv which we have named "multiphoton photochemical microplasma ignition." The mechanism for microplasma formation consists of three major components: (1) the multiphoton photochemical formation of oxygen atoms; (2) multiphoton ionization of these atoms to efficiently form free electrons in the laser focal volume and; (3) the formation of a laser microplasma using the electrons formed in the previous process. The liberated free electrons become the principal absorbers of laser radiation and serve as a heat sink. The laser focal volume (ignition kernel) is heated to a very high temperature such that the reactive gas mixture ultimately transitions into a flame front. The major difference between this and previous work on laser spark formation and gas ignition is that the multiphoton photochemical resonance ionization process provides a more efficient and controllable means of liberating free electrons

in the laser focal volume which leads to the laser spark formation. Lasers inherently possess certain attractive characteristics such as beam propagation through great distances, as well as excellent time-resolution.

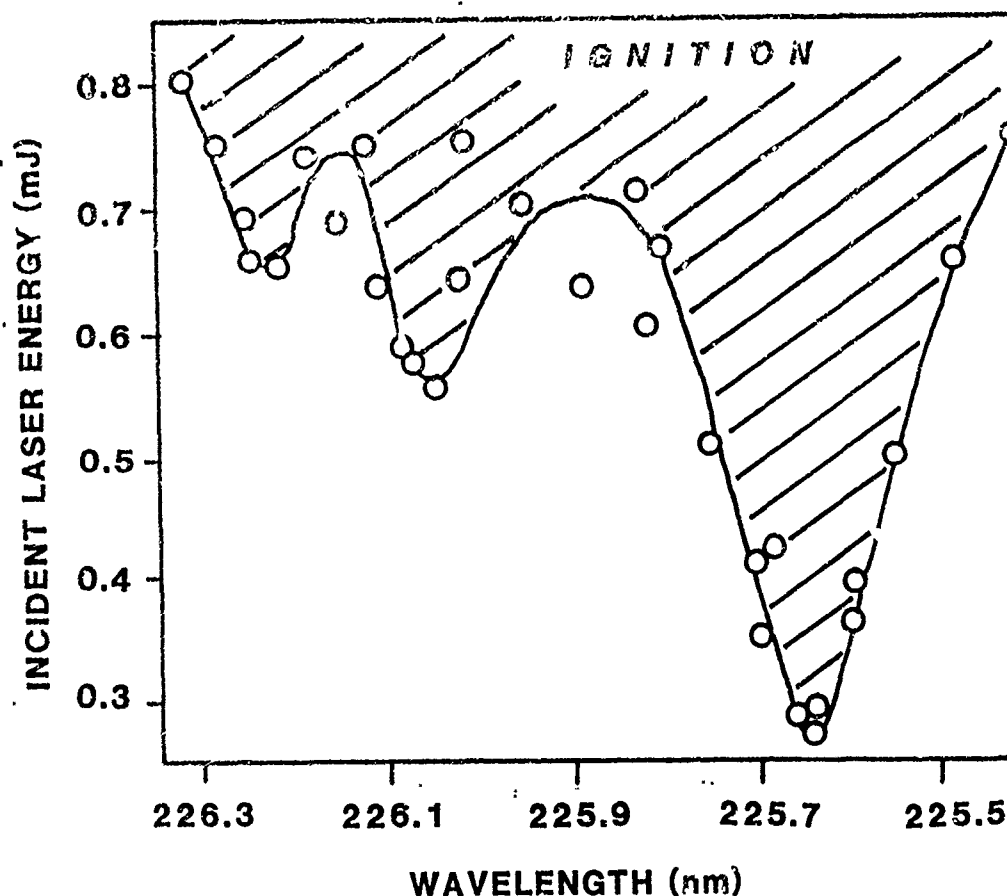


Figure 7. Plot of the Incident Laser Energy Required to Ignite a Premixed Flow of  $H_2/O_2$  as a Function of Laser Wavelength in the Region of 226 nm

#### B. H-Atoms

MPE. We have also been interested in the detection of hydrogen atoms (the smallest of atoms) because of its extreme importance in nearly every combustion environment and relevant chemical reactions. Many multiphoton excitation schemes have been implemented by various investigators to detect H atoms in a wide variety of flames,<sup>1,3,5,7,10,21</sup> see Figure 8. The first reported measurement of H atom concentrations in a flame by two-photon excited fluorescence was reported by Lucht, et al.,<sup>1</sup> in a premixed  $H_2/O_2/Ar$  low pressure flame (20 Torr), scheme 2, Figure 8. They used two-photon excitation of H atoms at 205 nm from the ground state level ( $n=1$ ) to the excited state level ( $n=3$ ). Laser induced fluorescence was then observed at 656.3 nm, which is the Balmer- $\alpha$  line because of  $n=3$  to  $n=2$  radiative decay. A decay rate of  $(3.7 \pm 0.4) \times 10^8 \text{ s}^{-1}$  was calculated from the tailing edge of the fluorescence

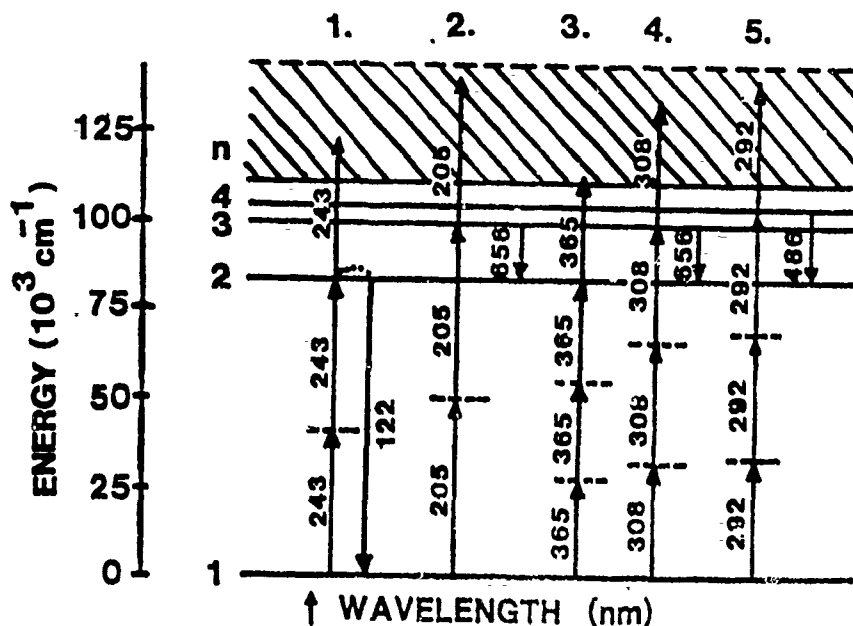


Figure 8. Simple Energy Level Diagram and Multiphoton Excitation Schemes for H Atoms. Energy on the vertical scale is given in wavenumbers. The arrows correspond to photon wavelengths.

pulse and a collisional quenching rate of about  $(2.7) \times 10^8 \text{ s}^{-1}$  was calculated at this pressure. Extrapolation of this low pressure result to atmospheric pressure gave a collisional quenching rate of  $10^{10} \text{ sec}^{-1}$ . We attempted to detect H atoms at this excitation wavelength in an atmospheric pressure flame. The dye laser second harmonic (Rhodamine 590) was mixed with the Nd:YAG fundamental and focused in a Raman cell. The first Anti-Stokes of the 224 nm beam in a  $\text{H}_2$  cell yielded  $\sim 50 \mu\text{J}$  of tunable laser radiation at 205 nm. No fluorescence signal was detected despite numerous attempts at this elevated pressure (a low pressure burner was not available in our laboratory at that time). This was attributed to the low laser energy which was available and strong quenching of the signal at atmospheric pressure which may dominate over radiative processes.

We attempted to use the three-photon excitation, scheme 4, Figure 8. Absorption of three photons at 308 nm from the  $n=1$  to the  $n=3$  state is followed by observation of emission at 656.3 nm. This particular wavelength is particularly attractive as a diagnostic technique since it coincidentally falls within the spectral gain of a XeCl excimer laser, wherein hundreds of mJ of laser energy are potentially available. However, we were not able to detect H atom emission since there was strong molecular interference from the hydroxyl radical (OH) which has single photon absorption at this wavelength region and also emits second order at 656.3 nm. A large ionization background from photoionization of OH precluded the use of the optogalvanic technique as a diagnostic tool.

H atoms were successfully detected in an atmospheric pressure  $\text{H}_2/\text{O}_2$  flame using scheme 5, Figure 8. Ground state H atoms were excited from the  $n=1$  to the  $n=4$  level through a three-photon absorption at 292 nm. Fluorescence

emission at 486 nm due to the  $n=4$  to the  $n=2$  radiative process (Balmer- $\beta$  emission) was detected. Figure 9a gives an excitation scan recorded as the uv laser was scanned through this three-photon resonance in a stoichiometric  $H_2/O_2$  atmospheric pressure flame while monitoring the emission with a monochromator/filter combination. The fluorescence emission spectrum was recorded by turning the excitation wavelength exactly to the maximum of the three-photon absorption and scanning the monochromator, Figure 9b. Alden, et al.,<sup>3</sup> have also utilized this excitation scheme and record the excitation scan point by point (so no estimate of the signal to noise ratio could be made). Furthermore, they noted a large background, both on and off resonance of the three-photon transition in the emission spectrum. Our signal to noise ratio was very good and we did not observe any appreciable laser induced background since we used a  $H_2/O_2$  flame and not an  $C_2H_2/O_2$  flame where there was laser-induced fluorescence from large hydrocarbons. We measured the laser power dependence for the three-photon excitation process. Five independent measurements were made and we obtained a value of  $n = 2.77 \pm 0.4$  for H atoms in the primary reaction zone. This measurement is consistent with the expected value of  $n=3$ . We found that the signal intensity was also highly sensitive to positioning within the flame front. Highly nonlinear power dependencies ( $n>5$ ) were obtained from very weak signals when the laser focal spot was translated slightly out of the primary reaction zone. This phenomenon is most likely attributable to photolysis of other flame species such as  $H_2O$  or  $OH$  to produce H atoms which were then three-photon excited. This process would probably require more than three photons. This excitation scheme may prove to be an excellent choice for diagnostic measurements of H atom profiles in combustion environments since strong fluorescence signals could be obtained quite easily (even at atmospheric pressure) and because of the convenient diagnostic wavelength available for the detection of the emission.

MPI. H atoms could also be detected using excitation scheme 3, Figure 8, in cold gaseous flows of  $H_2$  or  $D_2$  and in an atmospheric pressure  $H_2/O_2$  fuel rich flame. H atoms in the flame environment were excited through two-photon excitation from the ground state  $n=1$  to the lowest excited state  $n=2$ . For the two-photon excitation of H atoms at 243 nm there is no suitable analytical wavelength which is convenient for the detection of emission other than radiative decay back to the ground state with emission at 122 nm. However this radiation is largely absorbed by the flame gases as well as laboratory air in our experimental set up. An ideal diagnostic technique for H atoms using this excitation scheme would involve the optogalvanic probe since absorption of a third photon from the  $n=2$  level is sufficient to photoionize the atoms. However, the platinum electrode was damaged beyond repair due to the high temperature of the  $H_2/O_2$  flame and precluded its use in this particular experiment. We could induce multiphoton photolysis of the parent fuel in the preheat or post-flame gases in a combustion environment or cold flow of  $H_2$ , ionize the atoms and form a laser produced microplasma as had been demonstrated earlier in the discussion of O atom results. Within the high temperature plasma environment there exist collisional excitation and de-excitation processes which produce atomic hydrogen in the  $n=3$  excited state such that the radiative decay at 656.3 nm can be detected. This experiment was repeated with a flow of  $D_2$  and an isotopic blue shift of  $22 \text{ cm}^{-1}$  was observed in the excitation spectrum which is in excellent agreement with the well known value of  $22.4 \text{ cm}^{-1}$ . The temporal profile of the emission was indicative of a laser microplasma being produced (the full width at half

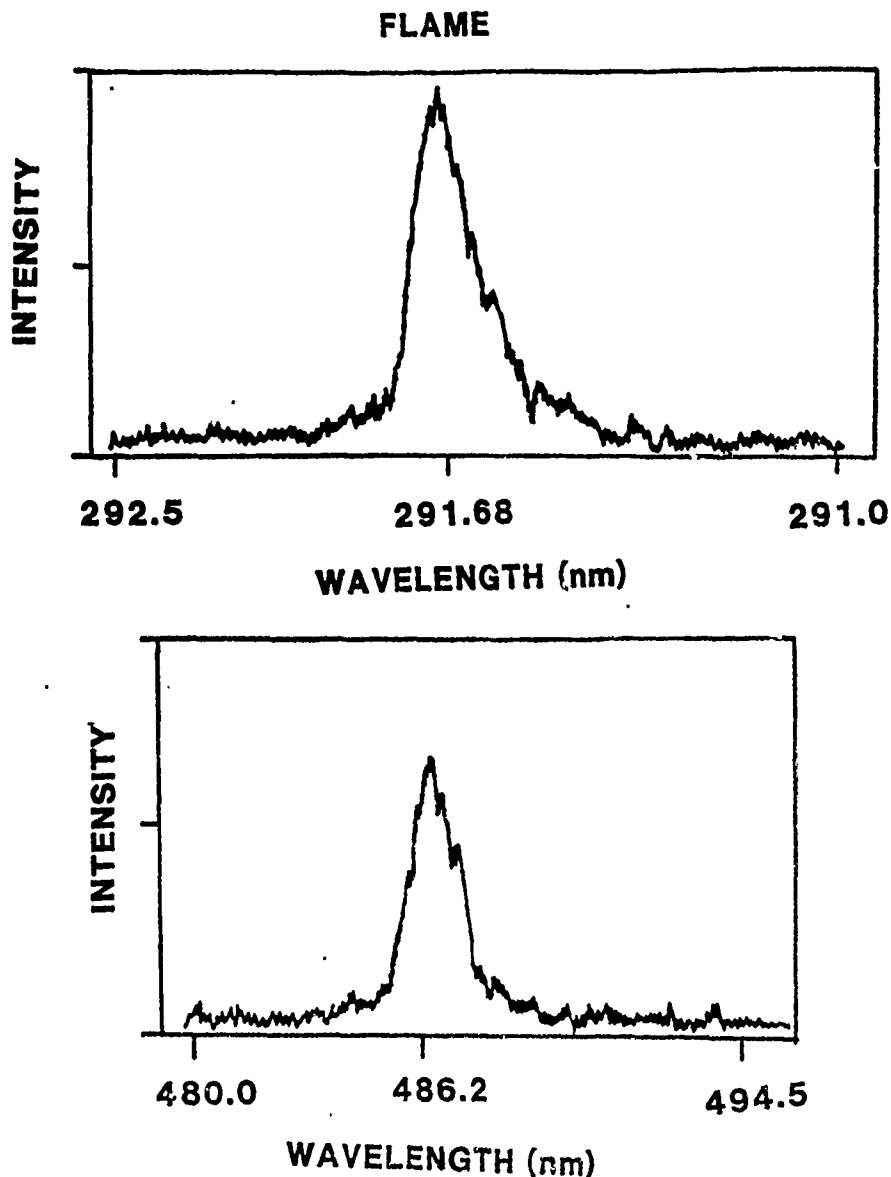


Figure 9. (a) Excitation Spectrum for H Atoms Using the Three-Photon Excitation ( $\lambda=272$  nm) Scheme 5 as Depicted in (b). The emission spectrum taken at 486 nm from the three-photon excitation process ( $\lambda=292$  nm) for H atoms.

maximum, FWHM, was  $\sim 70$  nsec). In order to gain information on the laser power dependence for the MPI process and without having a suitable ion detector available for atmospheric pressure measurements, we generated an H or D molecular beam with a hot wire filament in a time-of-flight mass spectrometer. Excitation spectra were recorded (Figure 10) by mass gating either the  $H^+$  or  $D^+$  signal with a boxcar integrator and then scanning the uv laser beam through the two-photon transition. Very strong ionization signals

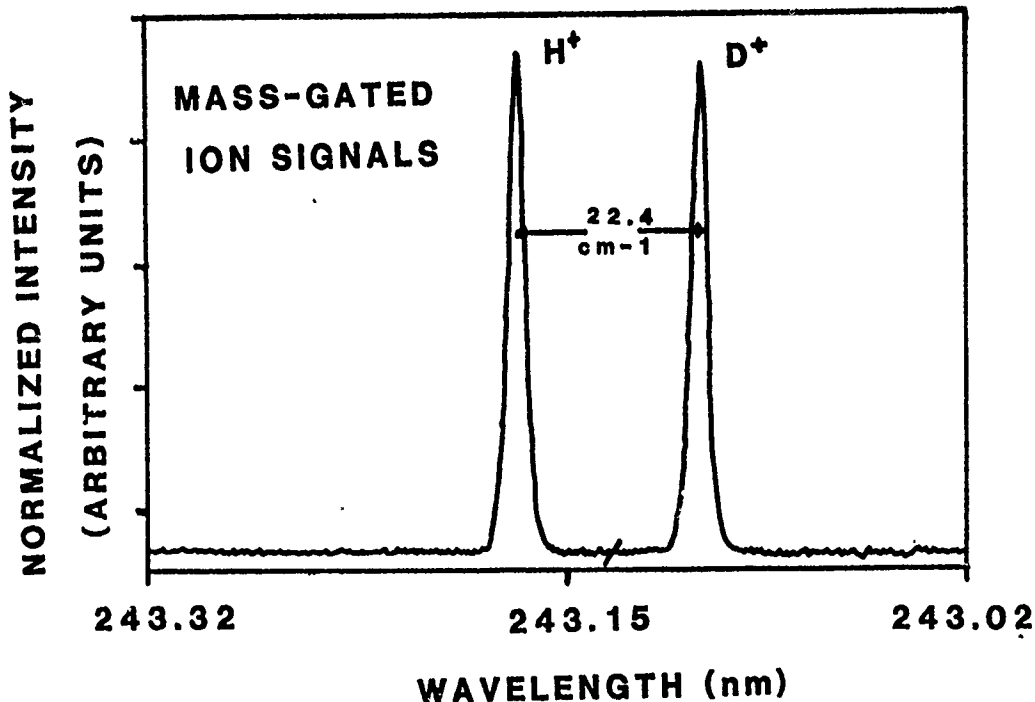


Figure 10. Mass-Gated Ion Signals (Excitation Spectrum) of  $H^+$  and  $D^+$  Taken in a Time-of-Flight Mass Spectrometer. An isotope of  $22.4 \text{ cm}^{-1}$  is evident. The slash (/) indicates the wavelength position where the mass gate was shifted from  $H^+$  to  $D^+$ .

(several volts) were seen using the dual microchannel plate detector (mcp) which was located at the top of a 1.5 m drift tube. A value of  $n = 2.75 \pm 0.2$  and  $2.63 \pm 0.3$  was obtained for H and D, respectively, corresponding to two-photon excitation and single photon ionization at low laser energies ( $< 0.5 \text{ mJ}$ ). These results clearly indicate that the overall excitation and ionization process was a three-photon process. As mentioned earlier, we could easily saturate the two-photon excitation step and record laser power dependencies of  $\sim 2.0$  for both H and D. We hope to be able to extend these measurements to a flame environment in the near future. Although the promise of the utilization of this two-photon scheme for fluorescence detection is limited, optogalvanic detection should yield excellent results. This is indicated in the results obtained by Tjossem and Cool<sup>7</sup> who excited the same H atom level,  $n=2$ , through a three-photon excitation and four-photon ionization at 365 nm using scheme 3, Figure 8. They report a sensitivity of  $< 1 \text{ ppm}$  for low pressure flames. They utilized an excimer-pumped dye laser system and generated the requisite 365 nm uv beam directly from the dye laser; thus eliminating the need to use frequency doubling and mixing techniques. They made no special attempt to maximize the spatial resolution capabilities of the method since the results appeared to be superior to the best efforts achievable by less direct methods. Alden was able to repeat Cool's work in a low pressure flame, but the corresponding experiment failed in an atmospheric pressure flame because of molecular interference from OH, as we had seen in our attempt at implementing the three-photon excitation scheme at 308 nm. We

will continue these experiments on H atom detection when the low pressure burner we are constructing is completed and a new tungsten optogalvanic probe is built.

### C. N- and C-Atoms

Here we will briefly discuss our first attempt at the detection of atomic nitrogen and carbon atoms in a combustion environment using tunable uv light. To the best of our knowledge, neither nitrogen atoms nor carbon atoms have ever been detected in a combustion environment using any optical diagnostic technique, although the nascent concentrations are expected to be much lower than that for H or O atoms. Nitrogen atoms were first detected utilizing a two-photon excitation scheme by Bischel, et al.<sup>17</sup> They produced ground-state N atoms in a low pressure microwave discharge then excited the atoms through a two-photon transition at 211 nm ( $2p^3 4S^0 + 2p^2 3p^4 D^0$ ). Fluorescence emission in the near infrared (869 nm) from the radiative process ( $2p^2 3p^4 D^0 + 2p^2 3s^4 P$ ) was detected. We tried to utilize this excitation technique to detect ground-state nitrogen atoms in atmospheric pressure fuel lean  $H_2/N_2O$  and  $CH_4/N_2O$  flames but the signal was swamped by background interference which remains unidentified. Furthermore, only  $\sim 40 \mu J$  of laser energy was obtained at 211 nm and the signal, if present at all, was probably heavily quenched. We also attempted to detect carbon atoms in an atmospheric pressure stoichiometric flame by generating tunable radiation in the wavelength region of 193 nm to excite carbon atoms from the metastable  $1D_2$  state to the  $1P^0_1$  at 193.1 nm. This metastable state may be formed through some elementary reaction rate process or by laser photolysis.<sup>22</sup> The production of tunable laser radiation in this wavelength region is described in the experimental section of this work. A suitable wavelength for the detection of the emission is the  $1P^0_1 + 1S_0$  radiative process at 247.9 nm. We obtained  $\sim 70 \mu J$  of tunable laser radiation but found that there were "holes" in the output of the uv beam as it was scanned throughout this wavelength region. It appears that absorption of molecular oxygen through the Schumann-Runge  $B^3\Sigma_u^- + X^3\Sigma_g^-$  band system bleached holes in the output profile of the laser beam. These are the dominant absorption bands for  $O_2$  and, unfortunately, the R(17) and P(15) absorption bands overlap exactly with the wavelength which corresponds to the carbon atom resonance at 193.1 nm.<sup>19</sup> Clearly if this wavelength is to be used as a diagnostic for C atoms, then the laser beam propagation pathway through the laboratory must be purged of  $O_2$ . An enclosed beam tube which is purged with an inert, non-absorbing gas at these wavelengths has recently been constructed in our laboratory.

### IV. CONCLUSION

We have investigated the potential utility of the application of multiphoton excitation processes for the detection of light atomic species such as O, H, N, and C atoms in combustion environments. Techniques which were utilized include multiphoton laser-induced fluorescence and ionization, the latter using an optogalvanic probe. Laser power dependencies were determined for most of the excitation schemes which were implemented. These measurements gave detailed information on the mechanism in the photoexcitation process such as the number of photons involved, potential photolytic effects which occurred therein and information on saturation effects. It was determined which of these schemes were most successful for the detection of each specific atom in a combustion environment. Clearly multiphoton

excitation is a viable approach for the detection of these light atomic species in combustion environments.

We discussed how the requisite high peak-powers that were utilized in the multiphoton excitation schemes could photochemically produce excess concentrations of atomic species (higher than that normally found in a combustion environment) and lead to erroneous concentration profile measurements. It was described how these photochemical perturbations could be used to augment combustion events such as ignition. This led to the discovery of a new ignition phenomenon which has been named "multiphoton photochemical microplasma ignition." The detailed steps involved in laser produced microplasmas have been determined and further laser ignition studies are currently under investigation.

A large amount of experimental data has been acquired using a very simple home-built atmospheric pressure burner. New sophisticated burner systems (low-pressure burner and strand burner) are under construction which will have mass-spectrometric analytical capabilities and a fourier transform infrared spectrometer, in addition to laser spectroscopic probes. The detection of these light atomic species in combustion environments by these various techniques will be used with flame models to unravel the detailed flame chemistry of the type of flame system of interest to our laboratory.

INTENTIONALLY LEFT BLANK.

## REFERENCES

1. R.P. Lucht, J.T. Salmon, G.B. King, D.W. Sweeney, and N.M. Laurendeau, "Two-Photon-Excited Fluorescence Measurement of Hydrogen Atoms in Flames," Optics Letters, Vol. 8, No. 7, pp. 365-367, July 1983.
2. M. Alden, H. Edner, P. Grafstrom, and S. Svanberg, "Two-Photon Excitation of Atomic Oxygen in a Flame," Optics Communications, Vol. 42, No. 4, pp. 244-246, July 1982.
3. M. Alden, A.L. Schawlow, S. Svanberg, W. Wendt, and P.L. Zhang, "Three-Photon-Excited Fluorescence Detection of Atomic Hydrogen in an Atmospheric-Pressure Flame," Optics Letters, Vol. 9, No. 6, pp. 211-213, June 1984.
4. J.E.M. Goldsmith, "Resonant Multiphoton Optogalvanic Detection of Atomic Oxygen in Flames," Journal of Chemical Physics, Vol. 78, No. 3, pp. 1610-1611, February 1983.
5. J.E.M. Goldsmith, "Resonant Multiphoton Optogalvanic Detection of Atomic Hydrogen in Flames," Optics Letters, Vol. 7, No. 6, pp. 437-438, July 1982.
6. J.E.M. Goldsmith, "Flame Studies of Atomic Hydrogen and Oxygen Using Resonant Multiphoton Optogalvanic Spectroscopy," Twentieth Symposium (International) on Combustion, The Combustion Institute, Pittsburgh, pp.1331-1335, 1984.
7. P.J.H. Tjossem and T.A. Cool, "Detection of Atomic Hydrogen in Flames by Resonance Optogalvanic Spectroscopy," Chemical Physics Letters, Vol. 100, No. 6, pp. 479-482, September 1983.
8. P. Lambropoulos, "Theory of Multiphoton Ionization: Near-Resonance Effects in Two-Photon Ionization," Physical Review A, Vol. 9, No. 5, pp. 1992-2013, May 1974.
9. G. Mainfray and C. Manus, "Resonance Effects in Multiphoton Ionization of Atoms," Applied Optics, Vol. 19, No. 23, pp. 3934-3940, December 1980.
10. U. Meier, K. Kohse-Hoinghaus, and Th. Just, "H and O Atom Detection for Combustion Applications: Study of Quenching and Laser Photolysis Effects," Chemical Physics Letters, Vol. 126, No. 6, pp. 567-573, May 1986.
11. A.W. Miziolek and M.A. DeWilde, "Multiphoton Photochemical and Collisional Effects During Oxygen-Atom Flame Detection," Optics Letters, Vol. 9, No. 9, pp. 390-392, September 1984.
12. C.J. Dasch and J.H. Bechtel, "Spontaneous Raman Scattering by Ground-State Oxygen Atoms," Optics Letters, Vol. 6, No. 1, pp. 36-38, January 1981.

13. R.E. Teets and J.H. Bechtel, "Coherent Anti-Stokes Raman Spectra of Oxygen Atoms in Flames," Optics Letters, Vol. 6, No. 10, pp. 458-460, October 1981.
14. B.E. Forch and A.W. Miziolek, "Oxygen-Atom Two Photon Resonance Effects in Multiphoton Photochemical Ignition of Premixed H<sub>2</sub>/O<sub>2</sub> Flows," Optics Letters, Vol. 11, No. 3, pp. 129-131, March 1986.
15. B.E. Forch and A.W. Miziolek, "Ultraviolet Laser Ignition of Premixed Gases by Efficient and Resonant Multiphoton Formation of Microplasmas", Combustion Science and Technology, Vol. 52, pp. 151-159, February 1987.
16. P.J. Dagdigian, B.E. Forch, and A.W. Miziolek, "Collisional Transfer Between and Quenching of the 3p <sup>3</sup>P and <sup>5</sup>P States of the Oxygen Atom," Chemical Physics Letters, Vol. 148, No. 4, pp. 299-308, July 1988.
17. W.K. Bischel, B.E. Perry, and D.R. Crosley, "Detection of Fluorescence from O and N Atoms Induced by Two-Photon Absorption," Applied Optics, Vol. 21, No. 8, pp. 1419-1429, April 1982.
18. S.W. Downey and R.S. Hozack, "Saturation of Three-Photon Ionization of Atomic Hydrogen and Deuterium at 243 nm," Optics Letters, Vol. 14, No. 1, pp. 15-17, January 1989.
19. M.P. Lee and R.K. Hanson, "Calculations of O<sub>2</sub> Absorption and Fluorescence at Elevated Temperatures for a Broadband Argon-Fluoride Laser Source at 193 nm," Journal of Quantitative Spectroscopy and Radiative Transfer, Vol. 36, No. 5, pp. 425-440, May 1986.
20. J.E.M. Goldsmith, "Photochemical Effects in Two-Photon Excited Fluorescence Detection of Atomic Oxygen Atoms in Flames", Applied Optics, Vol. 26, No. 17, pp. 3566-3572, September 1987.
21. T.W. Hansch, S.A. Lee, R. Wallenstein, and C. Wieman, "Doppler-Free Two-Photon Spectroscopy of Hydrogen 1S-2S\*," Physical Review Letters, Vol. 34, No. 6, pp.307-309, February 1975.
22. R.C. Sausa, A.J. Alfano, and A.W. Miziolek, "Efficient ArF Laser Production and Detection of Carbon Atoms from Simple Hydrocarbons," Applied Optics, Vol. 26, No. 17, pp. 3588-3593, September 1987.

<u>No of</u> <u>Copies</u>	<u>Organization</u>	<u>No of</u> <u>Copies</u>	<u>Organization</u>
1	Office of the Secretary of Defense OUSD(A) Director, Live Fire Testing ATTN: James F. O'Bryon Washington, DC 20301-3110	1	Director US Army Aviation Research and Technology Activity ATTN: SAVRT-R (Library) M/S 219-3 Ames Research Center Moffett Field, CA 94035-1000
2	Administrator Defense Technical Info Center ATTN: DTIC-DDA Cameron Station Alexandria, VA 22304-6145	1	Commander US Army Missile Command ATTN: AMSMI-RD-CS-R (DOC) Redstone Arsenal, AL 35898-5010
1	HQDA (SARD-TR) WASH DC 20310-0001	1	Commander US Army Tank-Automotive Command ATTN: AMSTA-TSL (Technical Library) Warren, MI 48397-5000
1	Commander US Army Materiel Command ATTN: AMCDRA-ST 5001 Eisenhower Avenue Alexandria, VA 22333-0001	1	Director US Army TRADOC Analysis Command ATTN: ATAA-SL White Sands Missile Range, NM 88002-5502
1	Commander US Army Laboratory Command ATTN: AMSLC-DL Adelphi, MD 20783-1145	(Class. only) 1	Commandant US Army Infantry School ATTN: ATSH-CD (Security Mgr.) Fort Benning, GA 31905-5660
2	Commander US Army, ARDEC ATTN: SMCAR-IMI-I Picatinny Arsenal, NJ 07806-5000	(Unclass. only) 1	Commandant US Army Infantry School ATTN: ATSH-CD-CSO-OR Fort Benning, GA 31905-5660
2	Commander US Army, ARDEC ATTN: SMCAR-TDC Picatinny Arsenal, NJ 07806-5000	1	Air Force Armament Laboratory ATTN: AFATL/DLODL Eglin AFB, FL 32542-5000  <u>Aberdeen Proving Ground</u>
1	Director Benet Weapons Laboratory US Army, ARDEC ATTN: SMCAR-CCB-TL Watervliet, NY 12189-4050	2	Dir, USAMSAA ATTN: AMXSY-D AMXSY-MP, H. Cohen
1	Commander US Army Armament, Munitions and Chemical Command ATTN: SMCAR-ESP-L Rock Island, IL 61299-5000	1	Cdr, USATECOM ATTN: AMSTE-TD
1	Commander US Army Aviation Systems Command ATTN: AMSAV-DACL 4300 Goodfellow Blvd. St. Louis, MO 63120-1798	3	Cdr, CRDEC, AMCCOM ATTN: SMCCR-RSP-A SMCCR-MU SMCCR-MSI
		1	Dir, VLAMO ATTN: AMSLC-VL-D

<u>No. of Copies</u>	<u>Organization</u>	<u>No. of Copies</u>	<u>Organization</u>
4	Commander US Army Research Office ATTN: R. Ghirardelli D. Mann R. Singleton R. Shaw P.O. Box 12211 Research Triangle Park, NC 27709-2211	2	Commander Naval Surface Warfare Center ATTN: R. Bernecker, R-13 G.B. Wilmot, R-16 Silver Spring, MD 20903-5000
2	Commander Armament RD&E Center US Army AMCCOM ATTN: SMCAR-AEE-B, D.S. Downs SMCAR-AEE, J.A. Lannon Picatinny Arsenal, NJ 07806-5000	5	Commander Naval Research Laboratory ATTN: M.C. Lin J. McDonald E. Oran J. Shnur R.J. Doyle, Code 6110 Washington, DC 20375
1	Commander Armament RD&E Center US Army AMCCOM ATTN: SMCAR-AEE-BR, L. Harris Picatinny Arsenal, NJ 07806-5000	1	Commanding Officer Naval Underwater Systems Center Weapons Dept. ATTN: R.S. Lazar/Code 36301 Newport, RI 02840
2	Commander US Army Missile Command ATTN: AMSMI-RK, D.J. Ifshin W. Wharton Redstone Arsenal, AL 35898	2	Commander Naval Weapons Center ATTN: T. Boggs, Code 388 T. Parr, Code 3895 China Lake, CA 93555-6001
1	Commander US Army Missile Command ATTN: AMSMI-RKA, A.R. Maykut Redstone Arsenal, AL 35898-5249	1	Superintendent Naval Postgraduate School Dept. of Aeronautics ATTN: D.W. Netzer Monterey, CA 93940
1	Office of Naval Research Department of the Navy ATTN: R.S. Miller, Code 432 800 N. Quincy Street Arlington, VA 22217	4	AL/LSCF ATTN: R. Corley R. Geisler J. Levine Edwards AFB, CA 93523-5000
1	Commander Naval Air Systems Command ATTN: J. Ramnarace, AIR-54111C Washington, DC 20360	1	AL/MKPB ATTN: B. Goshgarian Edwards AFB, CA 93523-5000
1	Commander Naval Surface Warfare Center ATTN: J.L. East, Jr., G-23 Dahlgren, VA 22448-5000	1	AFOSR ATTN: J.M. Tishkoff Bolling Air Force Base Washington, DC 20332
		1	OSD/SDIO/UST ATTN: L. Caveny Pentagon Washington, DC 20301-7100

<u>No. of Copies</u>	<u>Organization</u>	<u>No. of Copies</u>	<u>Organization</u>
1	Commandant USAFAS ATTN: ATSF-TSM-CN Fort Sill, OK 73503-5600	1	AVCO Everett Research Laboratory Division ATTN: D. Stickler 2385 Revere Beach Parkway Everett, MA 02149
1	F.J. Seiler ATTN: S.A. Shackelford USAF Academy, CO 80840-6528	1	Battelle Memorial Institute Tactical Technology Center ATTN: J. Huggins 505 King Avenue Columbus, OH 43201
1	University of Dayton Research Institute ATTN: D. Campbell AL/PAP Edwards AFB, CA 93523	1	Cohen Professional Services ATTN: N.S. Cohen 141 Channing Street Redlands, CA 92373
1	NASA Langley Research Center Langley Station ATTN: G.B. Northam/MS 168 Hampton, VA 23365	1	Exxon Research & Eng. Co. ATTN: A. Dean Route 22E Annandale, NJ 08801
4	National Bureau of Standards ATTN: J. Hastie M. Jacox T. Kashiwagi H. Semerjian US Department of Commerce Washington, DC 20234	1	Ford Aerospace and Communications Corp. DIVAD Division Div. Hq., Irvine ATTN: D. Williams Main Street & Ford Road Newport Beach, CA 92663
1	Aerojet Solid Propulsion Co. ATTN: P. Micheli Sacramento, GA 95813	1	General Applied Science Laboratories, Inc. 77 Raynor Avenue Ronkonkama, NY 11779-6649
1	Applied Combustion Technology, Inc. ATTN: A.M. Varney P.O. Box 17885 Orlando, FL 32860	1	General Electric Armament & Electrical Systems ATTN: M.J. Bulman Lakeside Avenue Burlington, VT 05401
2	Applied Mechanics Reviews The American Society of Mechanical Engineers ATTN: R.E. White A.B. Wenzel 345 E. 47th Street New York, NY 10017	1	General Electric Ordnance Systems ATTN: J. Mandzy 100 Plastics Avenue Pittsfield, MA 01203
1	Atlantic Research Corp. ATTN: M.K. King 5390 Cherokee Avenue Alexandria, VA 22314	2	General Motors Rsch Labs Physics Department ATTN: T. Sloan R. Teets Warren, MI 48090
1	Atlantic Research Corp. ATTN: R.H.W. Waesche 7511 Wellington Road Gainesville, VA 22065		

<u>No. of Copies</u>	<u>Organization</u>
2	Hercules, Inc. Allegheny Ballistics Lab. ATTN: W.B. Walkup E.A. Yount P.O. Box 210 Rocket Center, WV 26726
1	Honeywell, Inc. Government and Aerospace Products ATTN: D.E. Broden/ MS MN50-2000 600 2nd Street NE Hopkins, MN 55343
1	Honeywell, Inc. ATTN: R.E. Tompkins MN38-3300 10400 Yellow Circle Drive Minnetonka, MN 55343
1	IBM Corporation ATTN: A.C. Tam Research Division 5600 Cottle Road San Jose, CA 95193
1	IIT Research Institute ATTN: R.F. Remaly 10 West 35th Street Chicago, IL 60616
2	Director Lawrence Livermore National Laboratory ATTN: C. Westbrook M. Costantino P.O. Box 808 Livermore, CA 94550
1	Lockheed Missiles & Space Co. ATTN: George Lo 3251 Hanover Street Dept. 52-35/B204/2 Palo Alto, CA 94304
1	Los Alamos National Lab ATTN: B. Nichols T7, MS-B284 P.O. Box 1663 Los Alamos, NM 87545
1	National Science Foundation ATTN: A.B. Harvey Washington, DC 20550

<u>No. of Copies</u>	<u>Organization</u>
1	Olin Corporation Smokeless Powder Operations ATTN: V. McDonald P.O. Box 222 St. Marks, FL 32355
1	Paul Gough Associates, Inc. ATTN: P.S. Gough 1048 South Street Portsmouth, NH 03801-5423
2	Princeton Combustion Research Laboratories, Inc. ATTN: M. Summerfield N.A. Messina 475 US Highway One Monmouth Junction, NJ 08852
1	Hughes Aircraft Company ATTN: T.E. Ward 8433 Fallbrook Avenue Canoga Park, CA 91303
1	Rockwell International Corp. Rocketdyne Division ATTN: J.E. Flanagan/HB02 6633 Canoga Avenue Canoga Park, CA 91304
4	Sandia National Laboratories Division 8354 ATTN: R. Cattolica S. Johnston P. Mattern D. Stephenson Livermore, CA 94550
1	Science Applications, Inc. ATTN: R.B. Edelman 23146 Cumorah Crest Woodland Hills, CA 91364
3	SRI International ATTN: G. Smith D. Crosley D. Golden 333 Ravenswood Avenue Menlo Park, CA 94025
1	Stevens Institute of Tech. Davidson Laboratory ATTN: R. McAlevy, III Hoboken, NJ 07030

<u>No. of Copies</u>	<u>Organization</u>	<u>No. of Copies</u>	<u>Organization</u>
1	Thiokol Corporation Elkton Division ATTN: S.F. Palopoli P.O. Box 241 Elkton, MD 21921	1	California Institute of Technology ATTN: F.E.C. Culick/ MC 301-46 204 Karman Lab. Pasadena, CA 91125
1	Morton Thiokol, Inc. Huntsville Division ATTN: J. Deur Huntsville, AL 35807-7501	1	University of California Los Alamos Scientific Lab. P.O. Box 1663, Mail Stop B216 Los Alamos, NM 87545
3	Thiokol Corporation Wasatch Division ATTN: S.J. Bennett P.O. Box 524 Brigham City, UT 84302	1	University of California, San Diego ATTN: F.A. Williams AMES, B010 La Jolla, CA 92093
1	United Technologies ATTN: A.C. Eckbreth East Hartford, CT 06108	2	University of California, Santa Barbara Quantum Institute ATTN: K. Schofield M. Steinberg Santa Barbara, CA 93106
3	United Technologies Corp. Chemical Systems Division ATTN: R.S. Brown T.D. Myers (2 copies) P.O. Box 49028 San Jose, CA 95151-9028	1	University of Colorado at Boulder Engineering Center ATTN: J. Daily Campus Box 427 Boulder, CO 80309-0427
1	Universal Propulsion Company ATTN: H.J. McSpadden Black Canyon Stage 1 Box 1140 Phoenix, AZ 85029	2	University of Southern California Dept. of Chemistry ATTN: S. Benson C. Wittig Los Angeles, CA 90097
1	Veritay Technology, Inc. ATTN: E.B. Fisher 4845 Millersport Highway P.O. Box 305 East Amherst, NY 14051-0305	1	Case Western Reserve Univ. Div. of Aerospace Sciences ATTN: J. Tien Cleveland, OH 44135
1	Brigham Young University Dept. of Chemical Engineering ATTN: M.W. Beckstead Provo, UT 84058	1	Cornell University Department of Chemistry ATTN: T.A. Cool Baker Laboratory Ithaca, NY 14853
1	California Institute of Tech. Jet Propulsion Laboratory ATTN: L. Strand/MS 512/102 4800 Oak Grove Drive Pasadena, CA 91009	1	University of Delaware ATTN: T. Brill Chemistry Department Newark, DE 19711

<u>No. of Copies</u>	<u>Organization</u>	<u>No. of Copies</u>	<u>Organization</u>
1	University of Florida Dept. of Chemistry ATTN: J. Winefordner Gainesville, FL 32611	1	Polytechnic Institute of NY Graduate Center ATTN: S. Lederman Route 110 Farmingdale, NY 11735
3	Georgia Institute of Technology School of Aerospace Engineering ATTN: E. Price W.C. Strahle B.T. Zinn Atlanta, GA 30332	2	Princeton University Forrestal Campus Library ATTN: K. Brezinsky I. Glassman P.O. Box 710 Princeton, NJ 08540
1	University of Illinois Dept. of Mech. Eng. ATTN: H. Krier 144MEB, 1206 W. Green St. Urbana, IL 61801	1	Purdue University School of Aeronautics and Astronautics ATTN: J.R. Osborn Grissom Hall West Lafayette, IN 47906
1	Johns Hopkins University/APL Chemical Propulsion Information Agency ATTN: T.W. Christian Johns Hopkins Road Laurel, MD 20707	1	Purdue University Department of Chemistry ATTN: E. Grant West Lafayette, IN 47906
1	University of Michigan Gas Dynamics Lab Aerospace Engineering Bldg. ATTN: G.M. Faeth Ann Arbor, MI 48109-2140	2	Purdue University School of Mechanical Engineering ATTN: N.M. Laurendeau S.N.B. Murtiy TSPC Chaffee Hall West Lafayette, IN 47906
1	University of Minnesota Dept. of Mechanical Engineering ATTN: E. Fletcher Minneapolis, MN 55455	1	Rensselaer Polytechnic Inst. Dept. of Chemical Engineering ATTN: A. Fontijn Troy, NY 12181
3	Pennsylvania State University Applied Research Laboratory ATTN: K.K. Kuo H. Palmer M. Micci University Park, PA 16802	1	Stanford University Dept. of Mechanical Engineering ATTN: R. Hanson Stanford, CA 94305
1	Pennsylvania State University Dept. of Mechanical Engineering ATTN: V. Yang University Park, PA 16802	1	University of Texas Dept. of Chemistry ATTN: W. Gardiner Austin, TX 78712
		1	University of Utah Dept. of Chemical Engineering ATTN: G. Flandro Salt Lake City, UT 84112

No. of  
Copies

Organization

No. of  
Copies

Organization

- |   |  |
|---|--|
| 1 | Virginia Polytechnic<br>Institute and<br>State University<br>ATTN: J.A. Schetz<br>Blacksburg, VA 24061 |
| 1 | Freedman Associates<br>ATTN: E. Freedman<br>2411 Diana Road<br>Baltimore, MD 21209-1525                |

INTENTIONALLY LEFT BLANK.

## USER EVALUATION SHEET/CHANGE OF ADDRESS

This Laboratory undertakes a continuing effort to improve the quality of the reports it publishes. Your comments/answers to the items/questions below will aid us in our efforts.

1. BRL Report Number BRL--TR--3125 Date of Report JULY 1990

2. Date Report Received \_\_\_\_\_

3. Does this report satisfy a need? (Comment on purpose, related project, or other area of interest for which the report will be used.) \_\_\_\_\_  
\_\_\_\_\_  
\_\_\_\_\_

4. Specifically, how is the report being used? (Information source, design data, procedure, source of ideas, etc.) \_\_\_\_\_  
\_\_\_\_\_  
\_\_\_\_\_

5. Has the information in this report led to any quantitative savings as far as man-hours or dollars saved, operating costs avoided, or efficiencies achieved, etc? If so, please elaborate. \_\_\_\_\_  
\_\_\_\_\_  
\_\_\_\_\_

6. General Comments. What do you think should be changed to improve future reports? (Indicate changes to organization, technical content, format, etc.) \_\_\_\_\_  
\_\_\_\_\_  
\_\_\_\_\_  
\_\_\_\_\_

CURRENT  
ADDRESS

\_\_\_\_\_  
Name

\_\_\_\_\_  
Organization

\_\_\_\_\_  
Address

\_\_\_\_\_  
City, State, Zip Code

7. If indicating a Change of Address or Address Correction, please provide the New or Correct Address in Block 6 above and the Old or Incorrect address below.

OLD  
ADDRESS

\_\_\_\_\_  
Name

\_\_\_\_\_  
Organization

\_\_\_\_\_  
Address

\_\_\_\_\_  
City, State, Zip Code

(Remove this sheet, fold as indicated, staple or tape closed, and mail.)

-----FOLD HERE-----

**DEPARTMENT OF THE ARMY**

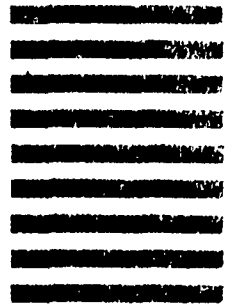
Director  
U.S. Army Ballistic Research Laboratory  
ATTN: SLCBR-DD-T  
Aberdeen Proving Ground, MD 21005-5066  
**OFFICIAL BUSINESS**



NO POSTAGE  
NECESSARY  
IF MAILED  
IN THE  
UNITED STATES

**BUSINESS REPLY MAIL**  
FIRST CLASS PERMIT No 0001, APG, MD

POSTAGE WILL BE PAID BY ADDRESSEE



Director  
U.S. Army Ballistic Research Laboratory  
ATTN: SLCBR-DD-T  
Aberdeen Proving Ground, MD 21005-9989

-----FOLD HERE-----